Electronic Supplementary Information

for

Mitigating Low-dimensional Phases and Defects with Methylammonium Chloride in High-Performance Dion-Jacobson Quasi-2D Tin Perovskite Solar Cells with Power Conversion Efficiency Over 6%

Chunqing Li,[a] Towhid H. Chowdhury,[a] Masahiro Yoshizawa-Fujita,[a] Masahiro Rikukawa,[a] Masatoshi Yanagida,[b] Yasuhiro Shirai[b] and Yuko Takeoka*[a]

Author address

[a] Faculty of Science and Engineering, Sophia University, 7-1 Kioi-cho, Chiyoda-ku, Tokyo 102-8554, Japan

[b] Photovoltaic Materials Group, Center for GREEN Research on Energy and Environmental Materials, National Institute for Materials Science (NIMS), 1-1 Namiki, Tsukuba, Ibaraki 305-0044, Japan

Corresponding Author

*E-mail: y-tabuch@sophia.ac.jp

Experimental

Materials

All chemicals were purchased from commercial suppliers and used as-received. Hydroiodic acid (HI; 57%), *N, N*-dimethylformamide (DMF), dimethylsulfoxide (DMSO) were purchased from Fujifilm Wako Pure Chemical, Ltd. Formamidinium iodide (FAI; 99.9%) was purchased from Luminiscent. *o*-Phenylenediamine (*o*-PDA, 99.5%), SnI_2, and SnF_2 were obtained from Sigma-Aldrich. Poly(3,4-ethylene dioxythiophene):poly(styrene sulfonate) (PEDOT:PSS) was obtained from Clevious. Phenyl-C61-butyric acid methyl ester (PCBM) was purchased from Kanto Chemical Co. Inc. Methylammonium chloride (MACl; 98%) and bathocuproine (BCP; 99%) were purchased from TCI.

Preparation

Synthesis of o-phenylenediammonium hydroiodide (o-PDAI$_2$): *o*-$PDAI_2$ was prepared by reacting an equivalent amount of *o*-PDA with hydroiodic acid in an ice bath. The solvent was removed after the reaction using a rotary evaporator. The obtained powder was washed with anhydrous ether. After drying under vacuum at 40 °C overnight, *o*-$PDAI_2$ was obtained as white crystals.

Preparation of perovskite precursor solution: Perovskite precursor solutions were prepared by dissolving *o*-$PDAI_2$ (0.2 mmol), FAI (0.6 mmol), SnI_2 (0.8 mmol), and SnF_2 (0.08 mmol) in 1 mL of DMSO overnight at room temperature. For MACl treated perovskites, MACl was additionally added to the perovskite precursor solution. PCBM solution was prepared by dissolving 20 mg of PCBM in 1 mL of anhydrous chlorobenzene (CB). Saturated BCP solution was prepared by dissolving 4 mg of BCP in 8 mL of anhydrous isopropanol. All the solutions were filtered using 0.45 µm syringe filters just prior to deposition to avoid unwanted particles in the precursor solution.

Device Fabrication

Photovoltaic cells were fabricated using pre-cleaned patterned indium tin oxide (ITO)-coated glass substrates (20 Ω square^{-1}). A thin hole-transporting layer of PEDOT:PSS was deposited onto an ITO substrate by spin-coating at 4000 rpm and subsequently drying at 150 °C for 20 min on a hot plate. The substrates were then transferred to an argon-filled glove box and the remaining steps were performed inside the glove box. The quasi-2D tin perovskite precursor was spin-coated on the substrate at 6000 rpm for 60 s (ramping slope 5 s) followed by dripping 150 mL of CB at 48 s after the start of spin-coating. To promote crystallization, the perovskite films were placed on a hot plate at 65 °C for 20 min and then at 100 °C for 10 min. PCBM was spin-coated on the film at 2000 rpm for 30 s and then annealed at 70 °C for 10 min to form the electron-transport layer. A thin BCP layer was spin-coated at 6000 rpm for 30 s, and was also annealed at 70 °C for 10 min. To complete the device fabrication, the samples were then transferred into an evaporation chamber for metal contact deposition. 100 nm of Ag was thermally evaporated at a pressure $<10^{-4}$ Pa.

Device characterization

The surface morphology and elemental analysis were evaluated from cross-sectional images of the quasi-2D tin perovskite films that were taken using high-resolution scanning electron microscopy (SEM, EDX; Hitachi, SU-8000) at an accelerating voltage of 5 kV. X-ray diffraction (XRD) patterns for the perovskite films were collected using an advanced X-ray diffractometer (Rigaku SmartLab, Cu Kα radiation, $\lambda = 1.5418$ Å). UV-vis absorption and photoluminescence (PL) spectra of the perovskite films were measured using a UV-vis spectrometer (Jasco, V-770) and a fluorescence spectrophotometer (Hitachi, F-7100), respectively. X-ray photoelectron spectroscopy (XPS) was conducted using a PHI 5000 Versa Probe II spectrometer. The performance of the photovoltaic cells was investigated at a scan rate of 0.04 V s^{-1} under 1 sun with AM 1.5G white light irradiation (100 mW cm^{-2}) using a source meter (Keithley, 2400) and a solar simulator (Peccell, PEC-L11). The light intensity was calibrated using a silicon (Si) diode (Bunkokeiki, BS-520BK). External quantum efficiency (EQE) spectra were measured using a spectrometer (Peccell, PEC-S15E).

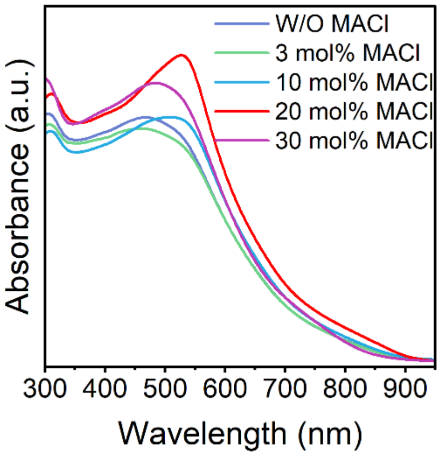

Figure S1. Full UV-vis absorption spectra (300-950 nm) of the quasi-2D tin perovskite with different concentrations of MACl.

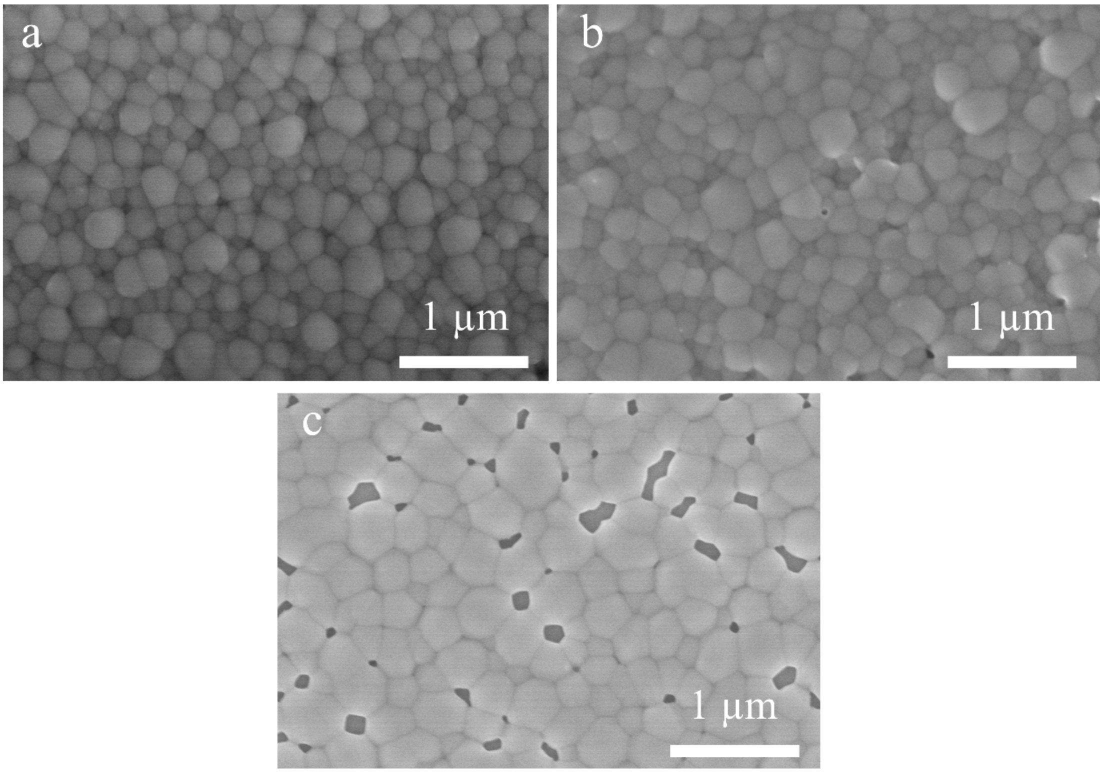

Figure S2. Surface SEM images of perovskite films with (a) 3 mol%, (b) 10 mol% and (c) 30 mol% MACl.

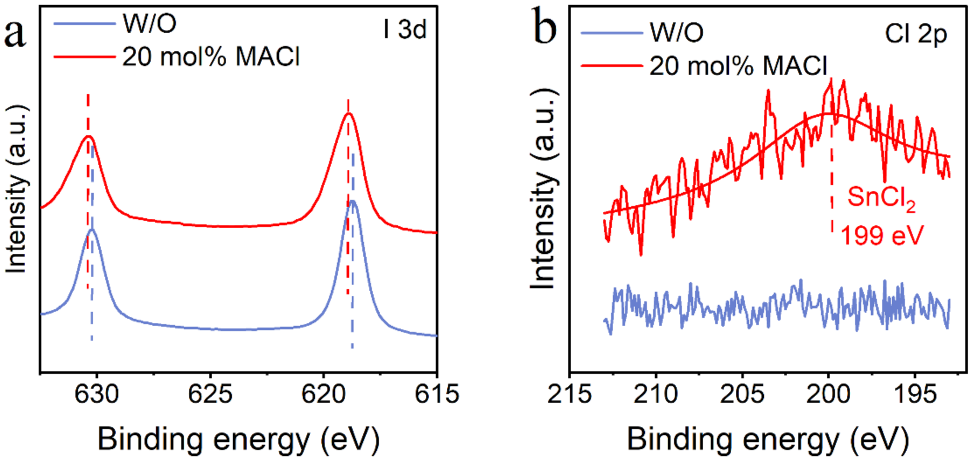

Figure S3. XPS spectra: (a) I 3d and (b) Cl 2p of the perovskite without and with 20 mol% MACl.

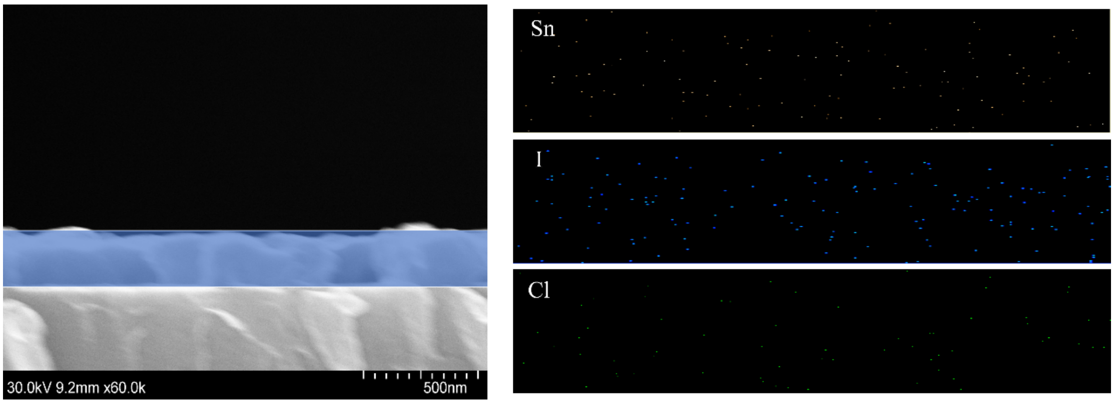

Figure S4. Cross-sectional SEM image (left) and EDX elemental maps (right) images of perovskite layers with 20 mol% MACl. The EDX maps were obtained from the green zone in the left image.

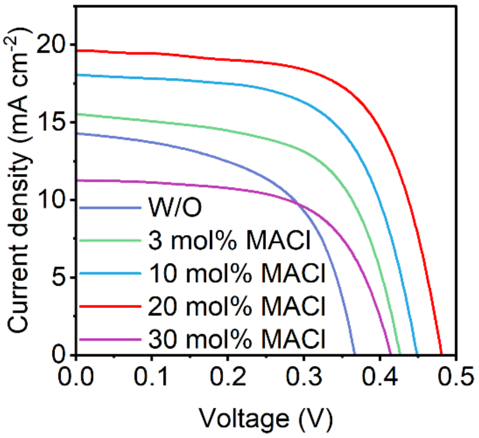

Figure S5. *J-V* curves for quasi-2D tin perovskite solar cells with various concentrations of MACl.

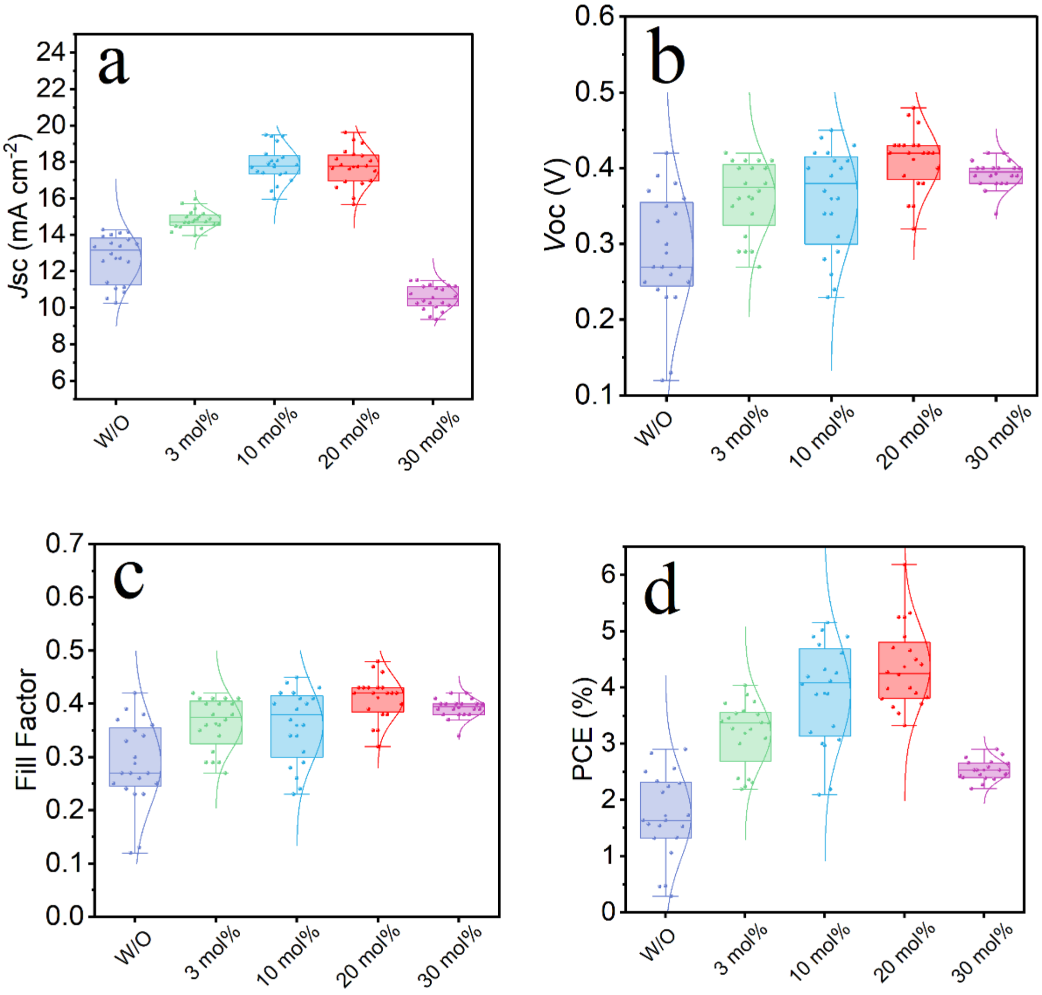

Figure S6. Statistics of device parameters for quasi-2D tin perovskite solar cells with pristine perovskite layer (W/O) and with various concentrations of MACl.

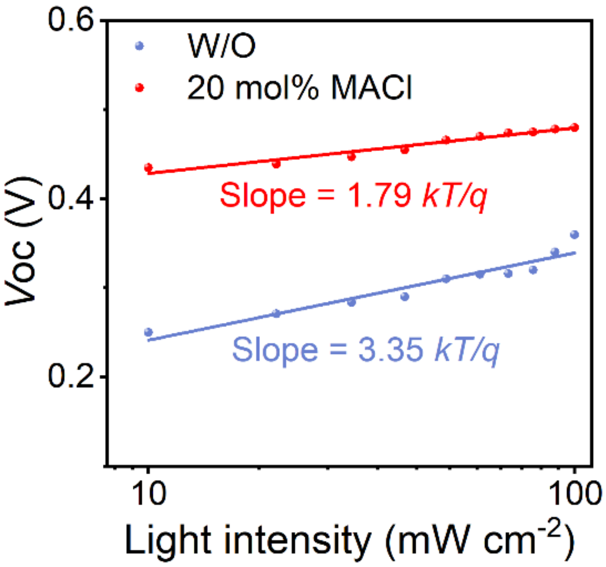

Figure S7. Seminatural-logarithmic plots of V_{OC} versus light intensity for quasi-2D tin perovskite solar cells with pristine perovskite layer (W/O) and with various concentrations of MACl.

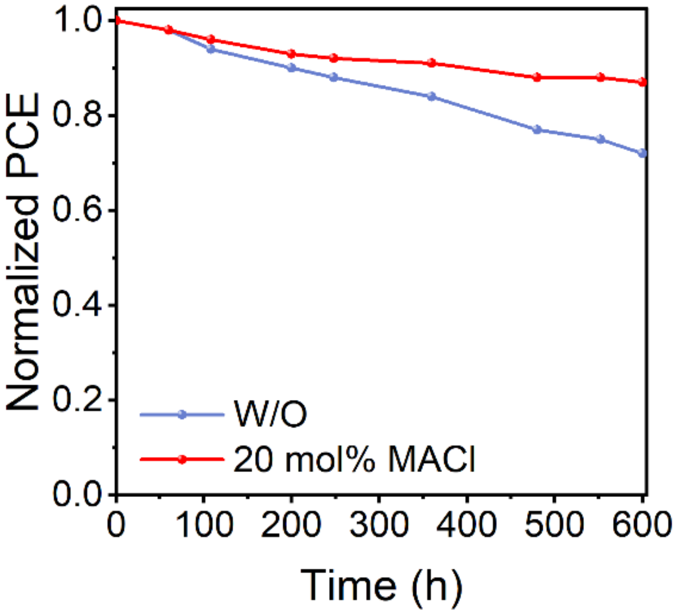

Figure S8. Long-term stability of quasi-2D tin perovskite solar cells with and without MACl, stored in Ar atmosphere and tested under ambient conditions.

Table S1. Parameters for devices with various concentrations of MACl.

Device	Scan direction	J_{sc} (mA/cm^2)	V_{oc} (V)	*FF*	*PCE* (%)
W/O	Forward	14.29	0.36	0.55	2.90
	Reverse	14.16	0.25	0.47	1.73
3 mol% MACl	Forward	15.55	0.42	0.60	4.04
	Reverse	15.22	0.37	0.54	3.00
10 mol% MACl	Forward	18.08	0.45	0.63	5.15
	Reverse	17.75	0.44	0.62	4.90
20 mol% MACl	Forward	19.62	0.48	0.66	6.20
	Reverse	19.22	0.47	0.58	5.25
30 mol% MACl	Forward	11.26	0.42	0.62	2.90
	Reverse	11.08	0.36	0.55	2.21